Safe Flight Envelope Uncertainty Quantification using Probabilistic Reachability Analysis

R. van den Brandt * **C.C. de Visser** **

* *Graduate Student, Department of Control and Simulation, Delft University of Technology, Kluyverweg 1 2629 HS Delft, The Netherlands.*
** *Assistant Professor, Department of Control and Simulation, Delft University of Technology, Kluyverweg 1 2629 HS Delft, The Netherlands.*

Abstract: Loss of Control is the primary contributor to aviation fatalities. To prevent these accidents, envelope protection is considered to be very effective. The calculation of the Safe Flight Envelope provides a bound on the states that can safely be approached by the aircraft. Although theoretically accurate, some states may not be reachable under the influence of disturbances (e.g. turbulence). In this paper a stochastic extension to the reachability analysis is applied to a simplified aircraft model. The probabilistic reachability analysis yields the transition probability from a state to the target set. By comparing the deterministic and probabilistic Safe Flight Envelope, it becomes clear that the Safe Flight Envelope can shrink considerably under the influence of turbulence. It is shown that for a $3\,\sigma$ (99.7 %) confidence interval, the envelope can shrink by as much as 50.8 % of the deterministic set. Furthermore, for high roll angles, some parts of the deterministic set have a 0 % transition probability under the influence of turbulence.

Keywords: Safe Flight Envelope, Reachability Analysis, Turbulence, Uncertainty Quantification, Probabilistic, Aircraft, Loss-of-Control, level-set, HJB

1. INTRODUCTION

According to a study by Boeing (2010) into commercial jet airplane accidents, more than 42 % of all aviation fatalities occur during Loss-of-Control (LOC) related accidents. LOC can occur when there is an unintended departure from controlled flight. Often, this happens when an aircraft leaves the normal flight envelope. This may result in a state from which recovery is hard or impossible (e.g. entering a stall or spin). Seventy-four LOC related accidents occurred in the last fifteen years among which were 27 stall accidents, 20 accidents with ice contaminated airfoils, and eight spatial disorientation accidents.

In search of methods to prevent LOC related accidents, flight envelope protection is often considered to be very effective (Lambregts et al. (2008)). Flight envelope protection consists of a human-machine interface that prevents the pilot from steering the aircraft into a state which exceeds the structural and aerodynamic operating limits. For such a system to be effective, knowledge of the flight envelope is required. The flight envelope, according to the standard definition, refers to a region of velocity and altitude or load-factor where the aircraft can operate safely. Since such an envelope only contains quasi-stationary states it is insufficient for the purpose of full envelope protection. A more comprehensive definition which also includes non-stationary states is known as the Safe Flight Envelope (SFE) (van Oort et al. (2011); Zhang et al. (2016); Lombaerts et al. (2013)). The SFE refers to the set of all states that can be reached, for which a return trajectory to the steady-state exists. It is formally defined as the intersection between the forwards and backwards reachable set. Computation of the reachable set is facilitated by making a connection between reachable set theory and the SFE (Lygeros (2004)).

Although the computed SFE is theoretically accurate, some states may be practically unattainable under the influence of disturbances. The presence of a disturbance could, for example, push the aircraft into a state outside the SFE so that it is unable to return to a steady-state. The main contribution of this paper is a new approach for flight envelope prediction from a probabilistic point of view that can quantify practical attainability. The stochastic counterpart of the reachability set theory will be used to compute the probabilistic SFE. By analyzing the differences between the deterministic and probabilistic SFEs, an assessment of the sensitivity of the SFE to disturbances can be made. We demonstrate our new approach using a widely used simplified aircraft model and show that current deterministic envelope prediction methods may produce dangerously optimistic results when neglecting the influence of disturbances.

2. SAFE FLIGHT ENVELOPE

The flight envelope commonly refers to a region that indicates the capabilities of an aircraft in terms of velocity and altitude or load-factor. Under nominal conditions the

aircraft should always be operated within these limits. When a flight envelope excursion happens, the aircraft can enter an upset condition from which it is hard or impossible to recover. Flight envelope protection is necessary (but not sufficient) for preventing the aircraft from leaving the flight envelope, thereby preventing LOC. Since the standard flight envelope only takes into account quasi-stationary states (e.g. coordinated turns or level flight) it does not provide bounds on dynamic maneuvers. To overcome the shortcomings of the standard flight envelope, a more complete representation of the flight envelope is required. The concept of a Safe flight Envelope (SFE) is introduced for the purpose of preventing LOC. It is formally stated as: *"The part of the state-space for which safe operation of the aircraft and safety of its cargo can be guaranteed, and externally posed constraints will not be violated"* (Van Oort (2011)).

The externally posed constraints are composed of the following envelope's:

- Dynamic Envelope: Envelope that is constrained by the dynamic behavior of the aircraft, due to its aerodynamics and kinematics.
- Structural and Comfort envelope: Constraints posed by the airframe, pilot, passengers and cargo. These constraints are usually defined through maximum accelerations and loads.
- Environmental Envelope: Constraints due to the environment in which the aircraft operates.

The constraints posed in the last two envelopes are well-known and can be quantified quite easily, however this is not true for the dynamic envelope. The main focus of this paper will be on the calculation of the dynamic envelope, where the complete envelope is given by the intersection of all three flight envelopes.

3. REACHABLE SET THEORY

The formal definition of the SFE provides a high level description, however this definition is not sufficient to facilitate computation of the SFE. For this purpose the SFE will be expressed in the framework of reachable set theory. Reachability set theory is widely used in safety analysis where the interest is in finding all states that can be reached, starting from a set of initial conditions, over a certain time horizon. In this section the connection with the reachable set theory will be made (Lygeros (2004)).

Consider a continuous-time dynamic system

$$\dot{\mathbf{x}}(t) = f(t, \mathbf{x}(t), \mathbf{u}(t)) \quad \mathbf{x} \in \mathbb{R}^n, \mathbf{u}(\cdot) \in \mathcal{U} \subseteq \mathbb{R}^m \qquad (1)$$

where $f(t, \mathbf{x}, \mathbf{u})$ is assumed to be Lipschitz continuous (i.e. $\dot{f}(t, \mathbf{x}, \mathbf{u}) < L$). With a time horizon $T \geq 0$ and a set of initial states $\mathcal{K} \subseteq \mathbb{R}^n$. A solution to the dynamic system is a trajectory through the state-space. The time horizon and the set of admissible control inputs ($\mathcal{U}$) provide a bound on the states that can be reached. A larger time horizon leads to a larger reachable set. Furthermore, when larger control inputs are permitted, a larger part of the state-space can be reached in the same amount of time. Based on the definition of the dynamical system given by (1), three different types of reachable sets can be defined.

- *Invariance:* $\mathcal{I}(t, \mathcal{K})$: Set of all states $\mathbf{x}(\cdot)$ for which there exists all the inputs $\mathbf{u}(\cdot) \in U_{[0,T]}$ such that $\mathbf{x}(t) \in \mathcal{K}$ for all $t \in [0, T]$.
- *Viability:* $\mathcal{V}(t, \mathcal{K})$: Set of all states $\mathbf{x}(\cdot)$ for which there exists at least one input $\mathbf{u}(\cdot) \in U_{[0,T]}$ such that $\mathbf{x}(t) \in \mathcal{K}$ for all $t \in [0, T]$.
- *Reachability:* $\mathcal{R}(t, \mathcal{K})$: Set of all the states $\mathbf{x}(\cdot)$ for which there exists at least one input $\mathbf{u}(\cdot) \in U_{[0,T]}$ and $t \in [0, T]$ such that $\mathbf{x}(t) \in \mathcal{K}$.

Fig. 1 provides an illustration of the different reachable kernels. The *invariance* set is the smallest set. It contains all states for which all possible control inputs keep the trajectory within $\mathcal{K}$ over the entire time horizon. Set $\mathcal{V}$ is the set of all states for which there exists at least one control sequence which keeps the trajectory within $\mathcal{K}$ over the entire time horizon. This set, together with the *invariance* set are completely contained inside the initial set $\mathcal{K}$. Finally, $\mathcal{R}$ is the set of all states for which there exists at least one control sequence that can steer the trajectory into set $\mathcal{K}$ within the time horizon. The definition of the *invariance*, *viability* and *reachability* kernel are used extensively in safety analysis (Lygeros (2004); Van Oort (2011); van Oort et al. (2011)).

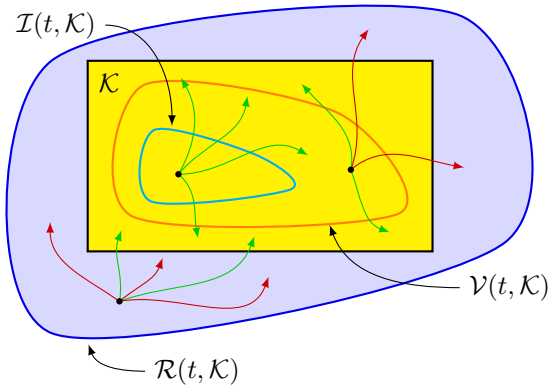

Fig. 1. Illustration of the different reachable kernels. Viability (orange), Invariance (cyan) and (backwards) reachability Set (Blue), Green: Successful trajectories; Red: Unsuccessful trajectories (Nabi (2016)).

The dynamic system (1) can be solved forwards in time, but also backwards in time which gives rise to two further types of reachability:

- *Forwards reachable Set:* $\mathcal{R}_f(t, \mathcal{K})$: Set of all the states $\mathbf{x}(\cdot)$ for which there exists a control input $\mathbf{u}(\cdot) \in U_{0,T}$ such that this set can be approached starting from the initial set $\mathcal{K}$ for $t \in [0, T]$.
- *Backwards Reachable Set:* $\mathcal{R}_b(t, \mathcal{K})$: Set of all the states $\mathbf{x}(\cdot)$ for which a control input $\mathbf{u}(\cdot) \in U_{[0,T]}$ exists at time $t \in [0, T]$, such that at least one state in the initial set $\mathcal{K}$ can be reached.

Fig. 2 shows both the forwards and backwards reachable set. For any state in the forwards reachable set, a trajectory towards this state exists, starting from somewhere in the initial set. The backwards reachable set consists of all the initial conditions for which a solution to the dynamic system exists that reaches the set $\mathcal{K}$. The SFE is defined as the intersection between the two. For any point inside

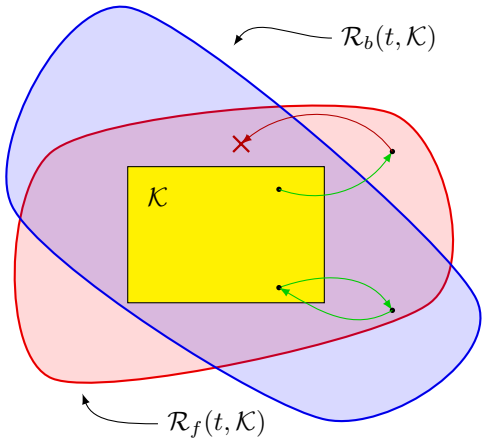

Fig. 2. SFE defined as the intersection between the forwards and backwards reachability set.

the SFE, there exists a trajectory from the initial set $\mathcal{K}$ to a state and back. If the state is in the forwards reachable set, but not in the backwards reachable set, it is possible to maneuverer to the state inside the forwards reachable set, but it is unable to return to the initial set.

4. OPTIMAL CONTROL FORMULATION

The *viability* and *invariant* sets as introduced in Section 3 can be linked to SUPMIN and INFMIN optimal control problems. The relation between the reachable sets and optimal control problems has been stated and proven by Lygeros (2004) and will be briefly summarized here.

Consider the continuous-time dynamic system

$$\dot{\mathbf{x}} = f(\mathbf{x}, t, \mathbf{a}, \mathbf{b}) \quad \mathbf{x} \in \mathbb{R}^n, \mathbf{a} \in \mathcal{A} \subseteq \mathbb{R}^{m_a}, \mathbf{b} \in \mathcal{B} \subseteq \mathbb{R}^{m_b} \tag{2}$$

where $\mathbf{a}$ and $\mathbf{b}$ are inputs to the system of differential equations. The inputs are considered to be two actors – pursuer and evader – with opposite goals. The pursuer tries to maximize the objective function while the evader tries to minimize it. This kind of problem is often referred to as a differential game. Solutions of the dynamic system (2) are trajectories of the system and will be denoted by (Mitchell et al. (2005))

$$\xi_f(\cdot; \mathbf{x}, t, \mathbf{a}, \mathbf{b}) \tag{3}$$

which satisfies the initial condition $\xi_f(0; \mathbf{x}, t, \mathbf{a}(\cdot), \mathbf{b}(\cdot)) = x_0$ and is differentiable almost everywhere

$$\frac{\mathrm{d}}{\mathrm{d}\tau}\xi_f(\tau; \mathbf{x}, t, \mathbf{a}, \mathbf{b}) = f\left(\xi_f(\tau; \mathbf{x}, t, \mathbf{a}, \mathbf{b}), \tau, \mathbf{a}(\tau), \mathbf{b}(\tau)\right) \tag{4}$$

Note the semi-colon to distinguish between the argument τ of ξ_f and the trajectory parameters.

The objective of the differential game is defined by a value function

$$V_1(\mathbf{x}, t) = \sup_{\mathbf{a}\in\mathcal{A}} \inf_{\mathbf{b}\in\mathcal{B}} \min_{\tau\in[0,T]} l\left(\xi(\tau; \mathbf{x}, t, \mathbf{a}, \mathbf{b})\right) \tag{5}$$

$$V_2(\mathbf{x}, t) = \inf_{\mathbf{a}\in\mathcal{A}} \sup_{\mathbf{b}\in\mathcal{B}} \min_{\tau\in[0,T]} l\left(\xi(\tau; \mathbf{x}, t, \mathbf{a}, \mathbf{b})\right) \tag{6}$$

V is called the value function or the cost-to-go. It represents the value of the solution to the optimal control problem at time t and initial state $\mathbf{x}$. The input $\mathbf{a}$ tries to maximize the minimum value attained by the function l along the state trajectory over the time horizon $[0, T]$ while the evader $\mathbf{b}$ tries to minimize this.

The *viability* and *invariant* sets can now be linked to the value function by (7,8)

$$\mathcal{V}(t, K) = \{\mathbf{x} \in \mathbb{R}^n | V_1(\mathbf{x}, t) > 0\} \tag{7}$$

$$\mathcal{I}(t, K) = \{\mathbf{x} \in \mathbb{R}^n | V_2(\mathbf{x}, t)) \geq 0\} \tag{8}$$

with $V(x, T) = l(x)$. An intuitive derivation can be made if it is assumed that the value function is differentiable. The value function can be reformulated as a Hamilton Jacobi Bellman (HJB) Partial Differential Equation (PDE) using Bellman's optimality Principle and a Taylor expansion of the value function (Van Oort (2011))

$$V_2(\mathbf{x}, t) = \inf_{\mathbf{a}\in\mathcal{A}} \sup_{\mathbf{b}\in\mathcal{B}} V\left(\xi_f\left(t + \Delta t; x, t, \mathbf{a}, \mathbf{b}\right), t + \Delta t\right) \tag{9}$$

First order Taylor expansion yields

$$V\left(\xi_f\left(t + \Delta t; x, t, \mathbf{a}, \mathbf{b}\right), t + \Delta t\right) \approx V(x, t) + V_t(x, t)\Delta t + V_x(x, t)\Delta x \tag{10}$$

Re-arranging the terms of (9) by the principle of optimality and dividing by Δt yields

$$\inf_{\mathbf{a}\in\mathcal{A}} \sup_{\mathbf{b}\in\mathcal{B}} \frac{V\left(\xi_f\left(t + \Delta t; x, t, \mathbf{a}, \mathbf{b}\right), t + \Delta t\right) - V(x, t)}{\Delta t} = 0 \tag{11}$$

Equation (11) can be thought of as one step/sub-problem of the dynamic programming principle.

Substituting the Taylor expansion into (11) yields

$$\inf_{\mathbf{a}\in\mathcal{A}} \sup_{\mathbf{b}\in\mathcal{B}} \frac{V_t(x, t)\Delta t + V_x(x, t) \cdot \Delta x}{\Delta t} = 0 \tag{12}$$

For the limit of $\Delta t \to 0$

$$\frac{\partial V_1}{\partial t}(\mathbf{x}, t) + \min\left\{0, \sup_{\mathbf{a}\in\mathcal{A}} \inf_{\mathbf{b}\in\mathcal{B}} \frac{\partial V_1}{\partial \mathbf{x}}(\mathbf{x}, t) f(\mathbf{x}, t, \mathbf{a}, \mathbf{b})\right\} = 0 \tag{13}$$

$$\frac{\partial V_2}{\partial t}(\mathbf{x}, t) + \min\left\{0, \inf_{\mathbf{a}\in\mathcal{A}} \sup_{\mathbf{b}\in\mathcal{B}} \frac{\partial V_2}{\partial \mathbf{x}}(\mathbf{x}, t) f(\mathbf{x}, t, \mathbf{a}, \mathbf{b})\right\} = 0 \tag{14}$$

The result is a PDE which includes an optimization over the inputs $\mathbf{a}$ and $\mathbf{b}$. The minimization term with zero guarantees that the reachable set cannot shrink as time marches forwards. A state that already entered the target set is restricted from leaving before the final time by 'freezing' the evolution of the trajectory (Zhang et al. (2016)).

Unfortunately, the assumption made in (9) that the value function is differentiable is often not valid, making it unable to interpret it as a solution in the 'classical' sense. Due to the switching of the optimal control and a discontinuity present in the right hand side of the HJB PDE the value function may not remain continuous. In order to obtain a solution to the HJB PDE a 'weak' formulation of solutions to these equations is necessary. Viscosity solutions form a general theory of 'weak' (i.e. non-differentiable) solutions. The interested reader is referred to Bressan (2011) for more information on viscosity solutions. Note that viscosity solutions are not the same as vanishing viscosity solutions which are the limit of an additional viscosity term for $\epsilon \to 0$.

5. PROBABILISTIC REACHABILITY ANALYSIS

Stochastic Differential Equations (SDEs) can be used to describe the behavior of a stochastic process. Instead of simulating each realization of the stochastic process, the forward Kolmogorov equation (or Fokker-Planck equation) can be used to describe the time rate of change of the Probability Density Function (PDF). Combining the optimal control framework with the time-evolution of the PDF will give rise to the field of probabilistic reachability analysis. The probabilistic reachability analysis will compute the transition probability to a certain state. Alternatively, the value function will be equal to the conditional probability of being in the initial set $\mathcal{K}$ at time $t = 0$ and in a final state X at time $t = T$.

Consider a controlled stochastic process $X^u_{t,x}$

$$\mathrm{d}X(s) = f(X(s), s, u(s))\mathrm{d}t + \sigma(X(s), s)\mathrm{d}W_s, \quad \forall s \in [t, T] \tag{15}$$

Let $\mathcal{K}$ be the non-empty target set in $\mathbb{R}^d$, $\rho \in [0, 1[$ and $t \leq T$. Consider the reachable set Ω_t under probability of success ρ, or the set of initial conditions x for which the probability that there exists a trajectory $X^u_{t,x}$ that reaches set $\mathcal{K}$ at time T, associated with the admissible control $u \in \mathcal{U}$ is at least ρ (Assellaou et al. (2015))

$$\Omega^\rho_t = \left\{x \in \mathbb{R}^d | \exists u \in \mathcal{U}, \mathbb{P}[X^u_{t,x}(T) \in \mathcal{K} > \rho]\right\} \tag{16}$$

Because the dynamics are stochastic, it is no longer possible to minimize the value function. Instead, the expected pay-off is minimized over all possible further realizations of the Wiener process (Kappen et al. (2011); Doya (2007)).

$$V(x,t) = \min_{\mathbf{u}\in\mathcal{U}} \{\mathbb{E}\left[V(x + \Delta f(x,u) + \xi, t + \Delta t)\right]\} \tag{17}$$

with $\xi \sim \mathcal{N}(0, \sigma(x,t))$ a process with normal distribution. The derivation is performed in a similar way as the deterministic case in Section 4. Taking the Taylor expansion of the value function by means of Itô's calculus. Since $\mathrm{d}x^2$ is of the order $\mathrm{d}t$ because of the Wiener process, the expansion must be performed up to the second order.

$$V(x + \Delta x, t + \Delta t) \approx V(x,t) + V_t(x,t)\Delta t + V_x(x,t)\Delta x + \frac{1}{2}\left(V_{xx}(x,t)\Delta x^2 + 2V_{xy}\Delta x\Delta t + V_{tt}(x,t)\Delta t^2\right) + \mathcal{O}(\delta^3) \tag{18}$$

where $\Delta x = \Delta f(x,t,u) + \xi$

Keeping all terms of order $\mathcal{O}(\Delta t)$

$$\mathbb{E}[V] = V(x,t) + \Delta f(x,u)V_x(x,t) + \frac{1}{2}\mathrm{Tr}(\sigma^2(x,t)V_{xx}(x,t)) \tag{19}$$

Substituting into (17) and dividing by Δt

$$\frac{V(x,t) - v(x,t+\Delta t)}{\Delta t} = \min_{\mathbf{u}\in\mathcal{U}} \left\{V_x f(x,t)^T + \frac{1}{2}\mathrm{Tr}(\sigma(x,t)\sigma(x,t)^T V_{xx})\right\} \tag{20}$$

For the limit of $\Delta t \to 0$ the value function is characterized by the viscosity solution to the stochastic HJB equation

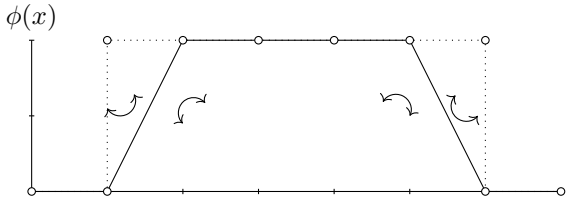

Fig. 3. Regularization of the indicator function.

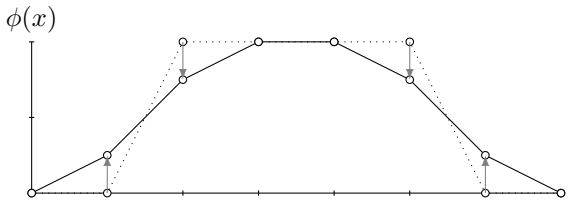

Fig. 4. Diffusion of the LS function.

$$\frac{\partial V}{\partial x}(x,t) + \inf_{u\in\mathcal{U}}\left\{\frac{\partial V}{\partial x}(x,t)f(x,t,u)\right\} + \frac{1}{2}\mathrm{Tr}\left\{\sigma(x,t)\sigma(x,t)^T\frac{\partial^2 V}{\partial x^2}(x,t)\right\} = 0 \tag{21}$$

The stochastic HJB equation can be solved using a similar method as for the deterministic HJB equation. Next to the convection term, an additional diffusion term is added to the Level-Set (LS) method. In contrary to the deterministic reachable set, the probabilistic reachable set is not represented by a zero level contour of the value function. Instead, the signed distance function is replaced by an indicator function.

$$\mathbb{1}_\mathcal{K}(x) = \begin{cases} 1 & \text{if } x \in \mathcal{K} \\ 0 & \text{if } x \notin \mathcal{K} \end{cases}$$

The initial condition of the LS function is then equal to one for all states that are inside the initial set $\mathcal{K}$, and all other states are equal to zero. Fig. 3 shows the indicator function as a dotted line. The regularization of the indicator function is shown as a solid line. Due to the discretization of the state-space, the LS function is slightly smaller which can introduce errors to the final solution. An error estimation is performed by Assellaou et al. (2015). The arrows in Fig. 3 represent the concavity of the implicit function. For a diffusion only problem, the second derivative, as found in the stochastic part of the HJB equation represents this concavity. Fig. 4 shows how the concavity of the LS function is related to the diffusion.

6. SIMPLIFIED AIRCRAFT MODEL

To analyze how external disturbances influence the SFE, a simplified aircraft model is considered. The deterministic SFE is calculated from the intersection of the forwards and backwards reachable set. Then, the probabilistic SFE is computed for the aircraft under influence of a suitable turbulence model.

6.1 Dynamic model

For the calculation of the SFE a nonlinear 3D simplified aircraft model will be considered (Lombaerts et al. (2013)). The dynamics of the model are

$$\dot{V} = -\frac{\rho S}{2m} V^2 C_{D_0} - g\sin(\gamma) + \frac{T}{m} - \frac{\rho S}{2m} V^2 (C_{D_\alpha}\alpha + C_{D_{\alpha^2}}\alpha^2) \quad (22)$$

$$\dot{\gamma} = -\frac{g}{V}\cos(\gamma) + \frac{\rho S}{2m} V (C_{L_0} + C_{L_\alpha}\alpha)\cos(\phi) - \frac{\rho S}{2m} V C_{Y_\beta}\beta\sin(\phi) \quad (23)$$

where $C_{L_\alpha} = 6.0723$, $C_{L_0} = 1.0656$, $C_{D_0} = 0.1599$, $C_{D_\alpha} = 0.5035$, $C_{D_{\alpha^2}} = 2.1175$, $m = 120\,000$ kg, $S = 260\,\mathrm{m}^2$ and $\rho = 1.225\,\mathrm{kg\,m^{-3}}$. The aerodynamic coefficients are based on the RCAM model (Looye and Bennani (1997)).

Both the thrust (T), the angle of attack (α) and the side-slip angle (β) are considered to be inputs to the system and are bounded. $\alpha \in [0; 14.5]°$, $\beta \in [-5, 5]°$ and $T \in [20\,546; 410\,920]$ N. Furthermore, the roll angle is threated as a discretely gridded input.

The maximizers for the Hamiltonian ($\hat{\alpha}$,$\hat{\beta}$ and $\hat{T}$) are

- If $p_1 > 0$ then $\hat{T} = T_{min}$ and
  - If $\hat{p} > \bar{\alpha}$ then $\hat{\alpha} = \alpha_{min}$
  - If $\hat{p} = \bar{\alpha}$ then $\hat{\alpha} = [\alpha_{min}; \alpha_{max}]$
  - If $\hat{p} < \bar{\alpha}$ then $\hat{\alpha} = \alpha_{max}$
- If $p_1 = 0$ then $\hat{T} \in [T_{min}; T_{max}]$ and
  - If $p_2 > 0$ then $\hat{\alpha} = \alpha_{min}$
  - If $p_2 = 0$ then $\hat{\alpha} \in [\alpha_{min}; \alpha_{max}]$
  - If $p_2 < 0$ then $\hat{\alpha} = \alpha_{max}$
- If $p_1 < 0$ then $\hat{T} = T_{max}$ and
  - If $\hat{p} \leq \alpha_{min}$ then $\hat{\alpha} = \alpha_{min}$
  - If $\alpha_{min} \leq \hat{p} \leq \alpha_{max}$ then $\hat{\alpha} = \hat{p}$
  - If $\hat{p} \geq \alpha_{max}$ then $\hat{\alpha} = \alpha_{max}$

besides, for the side-slip angle β holds

- If $p_2 \sin\phi > 0$ then $\hat{\beta} = \beta_{min}$
- If $p_2 \sin\phi = 0$ then $\hat{\beta} \in [\beta_{min}; \beta_{max}]$
- If $p_2 \sin\phi < 0$ then $\hat{\beta} = \beta_{max}$

where $\hat{p} = \frac{p_2 C_{L_\alpha}\cos\phi - p_1 V C_{D_\alpha}}{2 p_1 V C_{D_{\alpha^2}}}$ and $\bar{\alpha} = \frac{\alpha_{min}+\alpha_{max}}{2}$.

6.2 Safe Flight Envelope

The SFE as introduced in Section 3 is defined by the intersection of the forwards and backwards reachable set. These reachable sets are calculated by implementing the simplified aircraft model in the Level-Set Toolbox by Mitchell (2008). Fig. 5 shows the result of the reachability analysis starting from an initial set $V \in [55; 85]\,\mathrm{m\,s^{-1}}$ and $\gamma \in [-10; 10]°$ over a time horizon of 2 s. The forwards and backwards reachable set are shown in green and red respectively. The SFE is then computed by taking the intersection of both flight envelopes. Using the LS method, this is achieved by taking the maximum of both sets. The resulting intersection is marked in yellow. It can be seen that as the roll angle increases, the SFE becomes smaller. A similar trend can be seen for the flight path angle γ.

6.3 Probabilistic Safe Flight Envelope

For the probabilistic SFE the same model will be considered as for the deterministic SFE with the addition of a

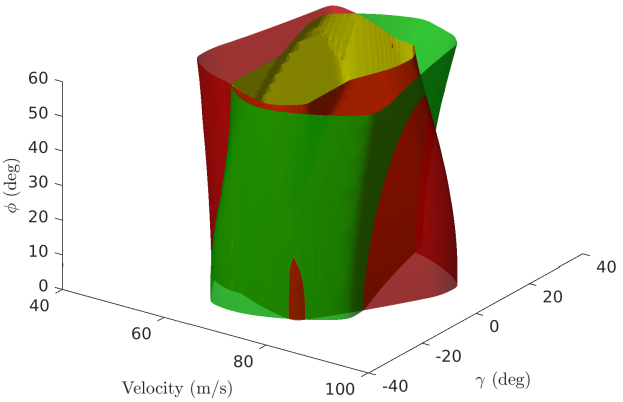

Fig. 5. Forward and Backward reachable set for the simplified aircraft model.

disturbance on the angle of attack (i.e. turbulence). The atmospheric turbulence for the simplified aircraft model is given by the Dryden spectra. For medium to high altitude turbulence, the turbulence scale length is chosen to be 500 m with a turbulence intensity of $2\,\mathrm{m\,s^{-1}}$ (MIL (1990)).

Then the gust angle of attack is calculated as

$$\alpha_{total} = \alpha + \alpha_g \quad (24)$$

$$\alpha_g = \tan^{-1}\left(\frac{w_g}{V}\right) \approx \frac{w_g}{V} \quad (25)$$

The dynamical model for the simplified aircraft now becomes

$$\dot{V} = -\frac{\rho S}{2m} V^2 C_{D_0} - g\sin(\gamma) + \frac{T}{m} - \frac{\rho S}{2m} V^2 (C_{D_\alpha}\alpha + C_{D_{\alpha^2}}\alpha^2) + W\frac{\rho S}{2m} V^2 C_{D_\alpha} \quad (26)$$

$$\dot{\gamma} = -\frac{g}{V}\cos(\gamma) + \frac{\rho S}{2m} V (C_{L_0} + C_{L_\alpha}\alpha)\cos(\phi) - \frac{\rho S}{2m} V C_{Y_\beta}\beta\sin(\phi) + W\frac{\rho S}{2m} V C_{L_\alpha} \quad (27)$$

Where W is the Brownian motion process representing the gust angle of attack. It should be noted that the noise terms with α^2 are left out in order to keep the control independent of the noise.

Fig. 6 shows the results of the probabilistic reachability analysis, starting from the same initial set $V \in [55; 85]\,\mathrm{m\,s^{-1}}$ and $\gamma \in [-10; 10]°$ over a time horizon of 2 s. The $1\,\sigma$ isosurfaces for the forwards and backwards reachable set are shown in green and red respectively. The $1\,\sigma$ confidence interval corresponds to all states with a 68.3 % reachability probability or higher. For the probabilistic reachability analysis, the SFE cannot be computed as the intersection of the two sets anymore. Instead, it is defined as the joint probability of the two sets (i.e. the probability to transition to a state and transition back to the initial set). For two independent processes this is equal to the product of the forwards transition probability with the backwards transition probability. Fig. 7 shows slices of the probabilistic SFE that give a better insight in how the probability changes with the states.

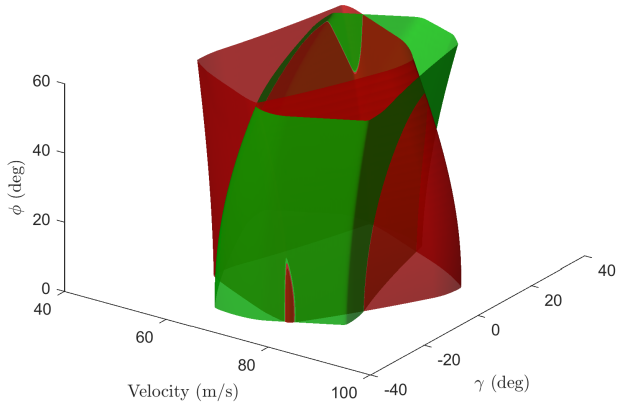

Fig. 6. Forwards and Backwards reachable set for the simplified aircraft model.

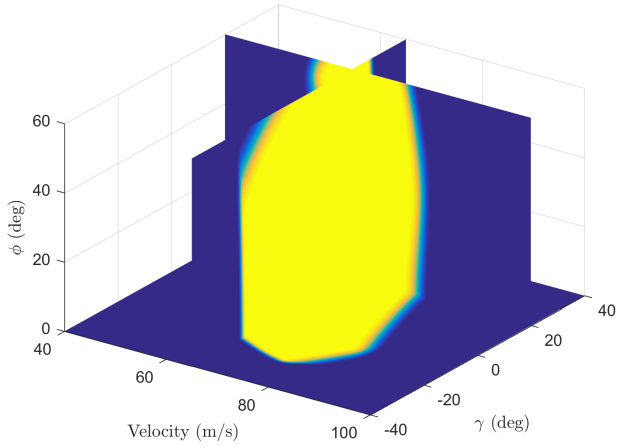

Fig. 7. Product of the forwards and backwards reachable set.

6.4 Sensitivity

The objective of this paper is to investigate the effect of disturbances on the SFE. By comparing the deterministic SFE with the confidence contours of the probabilistic SFE, it is possible to investigate the sensitivity. Since it is hard to compare the 3D reachable sets side-by-side, two slices have been made at roll angles of 0° and 60°.

Fig. 8 and Fig. 9 show both the deterministic SFE, as well as the probabilistic SFE. For the probabilistic SFE, the one, two and three σ isocontours are also plotted. The one, two and three σ isocontours represent the states in which a transition probability is achieved of at least 68.3 %, 95.5 % and 99.7 % respectively. Fig. 8 shows the results for a roll angle of 0°. The outer contour represents the deterministic SFE. It can be seen that the $1\,\sigma$ contour, which has a probability of 68.3 % is roughly the same size (slightly smaller) than the deterministic contour. This means that when the deterministic SFE is used for the purpose of LOC prevention in a setting with turbulence, there are some states that have a 31.7 % probability that the aircraft

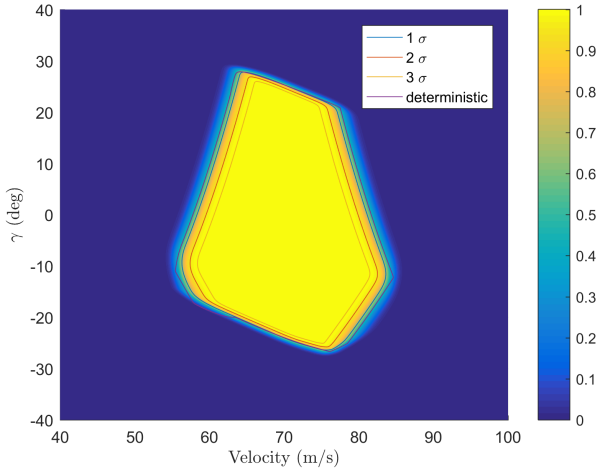

Fig. 8. SFE for a roll angle of 0°

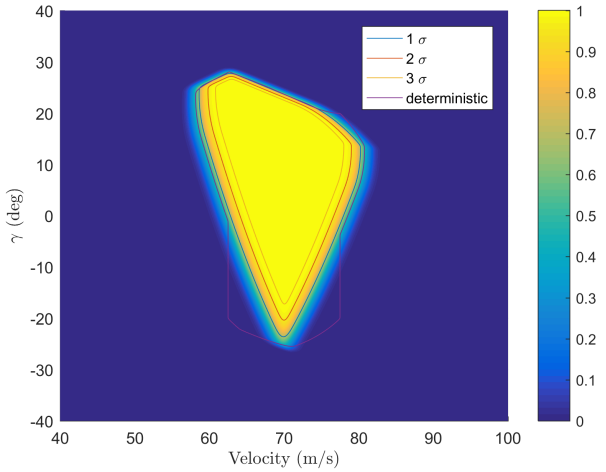

Fig. 9. SFE for a roll angle of 60°

Table 1. Size comparison between the deterministic and the probabilistic SFE.

Roll Angle/area	Deterministic	1σ	2σ	3σ
0°	100 %	94.3 %	81.9 %	71.4 %
30°	100 %	94.9 %	82.8 %	72.6 %
60°	100 %	78.0 %	62.8 %	50.8 %

cannot return to the initial set. The probabilistic SFE can be defined at an arbitrary probability as chosen by the operator to ensure safety of the aircraft and occupants. The $3\,\sigma$ contour is more suitable for preventing LOC as it gives a high probability of returning to the initial set, even in the presence of atmospheric turbulence. The difference between the deterministic and probabilistic SFE becomes more pronounced at higher roll angles. Fig. 9 shows the same information but now for a roll angle of 60°. It can be seen that the effect of disturbances on the SFE is greater. A fairly large part of the deterministic SFE has a transition probability of 0 %, which means that it is impossible for an aircraft which enters this part of the SFE to return to the initial set.

To get some more insight in the size difference of the deterministic compared to the probabilistic SFE, the relative

area between the deterministic set and the sigma contours is shown in Table 1. From this table it becomes clear that the disturbances have a greater effect on the SFE when the roll angle increases. For example, at a 60° roll angle, only 50 % of the deterministic SFE is enclosed by the $3\,\sigma$ contour.

7. VALIDATION

Generally, a Monte-Carlo method is employed to validate the results of the deterministic reachability analysis. This validation consists of a large number of individual trajectories which initial condition are located inside the initial set, for a number of (semi-) random control sequences. The reachable set is then approximated by the boundary of all trajectories. However, this approach is not suitable for application to the probabilistic reachability analysis. An alternative is presented as the Path Integral Monte Carlo (PIMC) method. The PIMC allows a step-by-step capture of the entire evolution of the response process in terms of PDF, starting from a known initial condition (deterministic or stochastic). The PIMC method has been used for a long time in physics to numerically solve the Fokker-Planck equation.

The starting point of the PIMC method is the Chapman-Kolmogorov equation (Pirrotta and Santoro (2011))

$$p_x(x, t+\tau) = \int_D p_x(x, t+\tau|\bar{x}, t) p_x(\bar{x}, t) d\bar{x} \qquad (28)$$

When the PDF is known at the current time step t, it is possible to evaluate the PDF after a small time step τ which holds true, because of the Markovian property of the response.

Fig. 10 illustrates the numerical solution to the Chapman-Kolmogorov equation for a single point. The blue line represents the (Gaussian) distribution of the SDE at the current time t. This distribution is denoted by $p_x(x, t)$. The PIMC method samples the SDE over the domain D. Fig. 10 shows these samples for a single point denoted by $\bar{x}$. The gray samples are all unique realizations of the SFE starting from $\bar{x}$ over a time horizon τ. The PDF corresponding to these samples is shown in cyan and is denoted $p_x(x, t+\tau|\bar{x}, t)$. The PDF belonging to $\bar{x}$ ($p_x(x, t+\tau|\bar{x}, t)$) is then weighted by the previous probability at $p(\bar{x}, t)$. The PDF at the next time instant $(t+\tau)$ is shown in red. This PDF is the ensemble of all local Gaussian probability distributions over the domain D.

To check that the aircraft model was correctly implemented in the LS toolbox, a validation is performed for the simplified aircraft model. In this validation the backwards reachability for two cases is considered, a roll angle of 0° and 60°. The difference between the LS and PIMC method is shown in Fig. 11 and Fig. 12 for a roll angle of 0° and 60° respectively. The reachability is calculated over a time horizon of 2 s, starting from an initial set as represented by the black rectangle.

From the validation it becomes clear that the LS solution is similar to the PIMC method. When looking at the magnitude of the transition probability, a slight difference can be seen in the corners of the PIMC method, However, the PIMC solution always produces a similar or lower estimation of the transition probability, as expected.

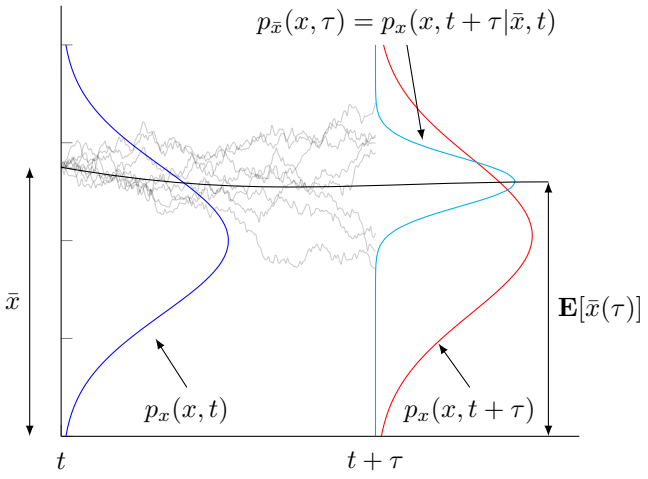

Fig. 10. Path Integral Monte Carlo method.

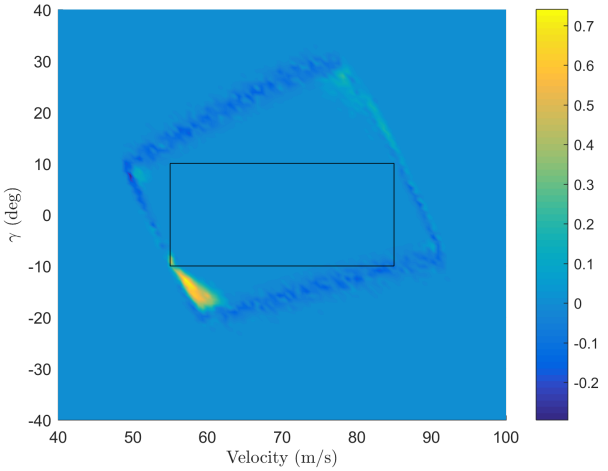

Fig. 11. Difference between the PIMC and the LS solution for $\phi = 0°$.

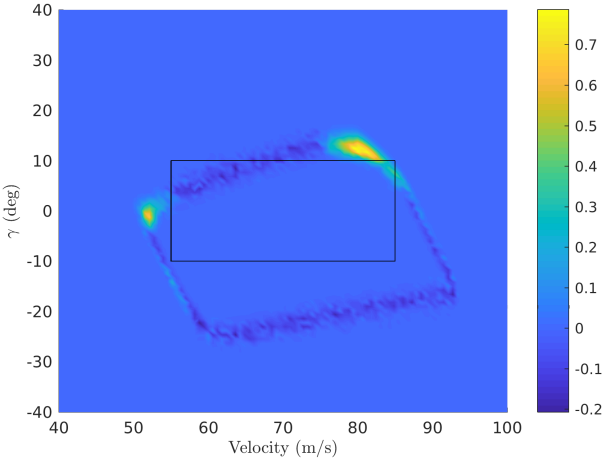

Fig. 12. Difference between the PIMC and the LS solution $\phi = 60°$.

8. CONCLUSION

In this paper, the reachability analysis which is commonly used to computed the Safe Flight Envelope (SFE), is extended to quantify the reachability probability of stochastic processes. This set is referred to as the probabilistic reachable set and describes the transition probability of a Stochastic Differential Equation (SDE) to a target set. The conditional probability between the forwards and backwards probabilistic reachable set then yields the probabilistic SFE. The difference between the deterministic and probabilistic SFE is analyzed for a simplified aircraft model.

When comparing the deterministic SFE with the probabilistic counterpart, it becomes clear that the deterministic envelope roughly corresponds to the $1\,\sigma$ isocontour. This means that for most states in the deterministic SFE there is a 68.3 % or higher probability of returning to the initial set. In most scenarios, a $1\,\sigma$ reachability probability is not acceptable. A better suited definition would be the $3\,\sigma$ contour. This contour contains all states for which the transition probability is at least 99.7 %. The deterministic SFE is significantly smaller than the $3\,\sigma$ contour. When comparing the area of both envelopes at different roll angles it can be observed that the stochastic envelope ranges from 71.4 % till 50.8 % of the area. This means that at large roll angles the SFE is almost half that of the case without disturbances. Furthermore, for some states in the deterministic SFE, the transition probability under influence of external turbulence is 0 %, meaning that there is no possibility of returning to the initial set.

Finally, validation of the probabilistic reachable set is performed by means of a Path Integral Monte Carlo method. When looking at the magnitude of the transition probability, a slight difference can be seen in the corners of the Path Integral Solution. However, the Path Integral Monte Carlo method always produces a similar or lower estimation of the transition probability, as expected.

REFERENCES

(1990). *Flying Qualities of Piloted Vehicles*. Department of Defense. MIL-STD-1797A.

Assellaou, M., Bokanowski, O., and Zidani, H. (2015). Error estimates for second order hamilton-jacobi-bellman equations. approximation of probabilistic reachable sets. *Discrete and Continuous Dynamical Systems-Series A (DCDS-A)*, 35(9), 3933–3964.

Boeing, J. (2010). Statistical summary of commercial jet airplane accidents worldwide operations 1959–2009. Technical report, Technical Report, Aviation Safety Boeing Commercial Airplanes, Seattle, Washington 98124-2207, USA.

Bressan, A. (2011). Viscosity solutions of hamilton-jacobi equations and optimal control problems. *Lecture notes*.

Doya, K. (2007). *Bayesian brain: Probabilistic approaches to neural coding*. MIT press.

Kappen, H.J. et al. (2011). Optimal control theory and the linear bellman equation. *Inference and Learning in Dynamic Models*, 363–387.

Lambregts, A., Nesemeier, G., Wilborn, J., and Newman, R. (2008). Airplane upsets: Old problem, new issues. In *AIAA Modeling and Simulation Technologies Conference and Exhibit*, 6867.

Lombaerts, T., Schuet, S., Wheeler, K., Acosta, D.M., and Kaneshige, J. (2013). Safe maneuvering envelope estimation based on a physical approach. In *AIAA Guidance, Navigation, and Control (GNC) Conference*, 4618.

Looye, G. and Bennani, S. (1997). Description and analysis of the research civil aircraft model (rcam). *Technical publication TP-088-27, Group for Aeronautical Research and Technology in EURope (GARTEUR)*.

Lygeros, J. (2004). On reachability and minimum cost optimal control. *Automatica*, 40(6), 917–927.

Mitchell, I.M. (2008). The flexible, extensible and efficient toolbox of level set methods. *Journal of Scientific Computing*, 35(2), 300–329.

Mitchell, I.M., Bayen, A.M., and Tomlin, C.J. (2005). A time-dependent hamilton-jacobi formulation of reachable sets for continuous dynamic games. *IEEE Transactions on automatic control*, 50(7), 947–957.

Nabi, H. (2016). *Effects of Structural Failures on the Safe Flight Envelope of Aircraft*. Master's thesis, TU Delft, Delft University of Technology.

Pirrotta, A. and Santoro, R. (2011). Probabilistic response of nonlinear systems under combined normal and poisson white noise via path integral method. *Probabilistic Engineering Mechanics*, 26(1), 26–32.

Van Oort, E.R. (2011). *Adaptive backstepping control and safety analysis for modern fighter aircraft*. TU Delft, Delft University of Technology.

van Oort, E., Chu, Q., and Mulder, J.A. (2011). Maneuver envelope determination through reachability analysis. In *Advances in Aerospace Guidance, Navigation and Control*, 91–102. Springer.

Zhang, Y., de Visser, C.C., and Chu, Q.P. (2016). Online safe flight envelope prediction for damaged aircraft: A database-driven approach. In *AIAA Modeling and Simulation Technologies Conference*, 1189.